Chapter 8 Protection Measures for Navigational Channels

8. Protection Measures for Navigational Channels

8.1 Sediment Transport at Each Channel

The type of sediment transport in 26 channels facing the sea under the management of CDCⅡ is summarized in Table 8.1-1.

Table 8.1-1 Classification of Navigational Channels with respect to Sediments Characteristics

Volume of Sediments	**Source of Sediments**		
	Longshore Drift		**River/Lake**
	Predominant Direction S → N	**Predominant Direction N → S**	
Large 10^5 m^3/year | 10^4 m^3/year	**Type A** (With Jetty) • Bang Ra Pha • Tanyong Pao • Panare • Bang Maruat	None	**Type E** (With Jetty) • Songkhla • Pattani (Without Jetty) • Pak Phanang
Medium 10^4 m^3/year | 10^3 m^3/year	**Type B** (With Jetty) • Na Thap • Sakom • Thepha • Sai Buri • Narathiwat (Without Jetty) • Sai Samo • Bang Ta Wa • Ta Lo Lae Weng	**Type C** (With Jetty) • Sichon • Tha Sala (Without Jetty) • Khlong Tung Ca • Tha Mak • Pak Duat	**Type F** (Without Jetty) • Pak Phaying • Pak Phun • Pak Paya • Pak Nakhon
Small less than 10^3 m^3/year	None	**Type D** (Without Jetty) • Khanom	**Type G** (Without Jetty) • Ru Sa Mi Lae

8.2 Coastal Changes due to Training Jetties

8.2.1 Analysis for Amount of Deposition and Erosion by Topographic Survey (In Case of Bang Ra Pha)

The shoreline changes after construction of jetties in Bang Ra Pha, which was completed in June 1999, show that a huge deposition area appears in the east part of the jetties and a large erosion area in the west part (see Figure 8.2.1-1).

In this coastal area, topographic and bathymetric survey was newly carried out at 50 to 100 m intervals along the shorelines in September 2001 during the second phase study. In addition, there is an existing topographic and bathymetric map surveyed in 1996 before the construction of jetties in this area.

The amount of deposition and erosion near the jetties by topographic changes due to the construction of jetties in Bang Ra Pha area was calculated in comparison with the above-mentioned maps along the survey lines shown in Figure 8.2.1-2.

Calculation results show that the amount of deposition at east side of jetties is 44,625 m^3 between survey lines No. E-2 and No. E-10 and the amount of erosion at west side of jetties is 31,375 m^3 between survey lines No. W-2 and No. W-10 (see Table 8.2.1-1, and Figure 8.2.1-3).

East ←

West →

(taken on March 27, 2001)

Figure 8.2.1-1 Aerial Photo of Bang Ra Pha Area

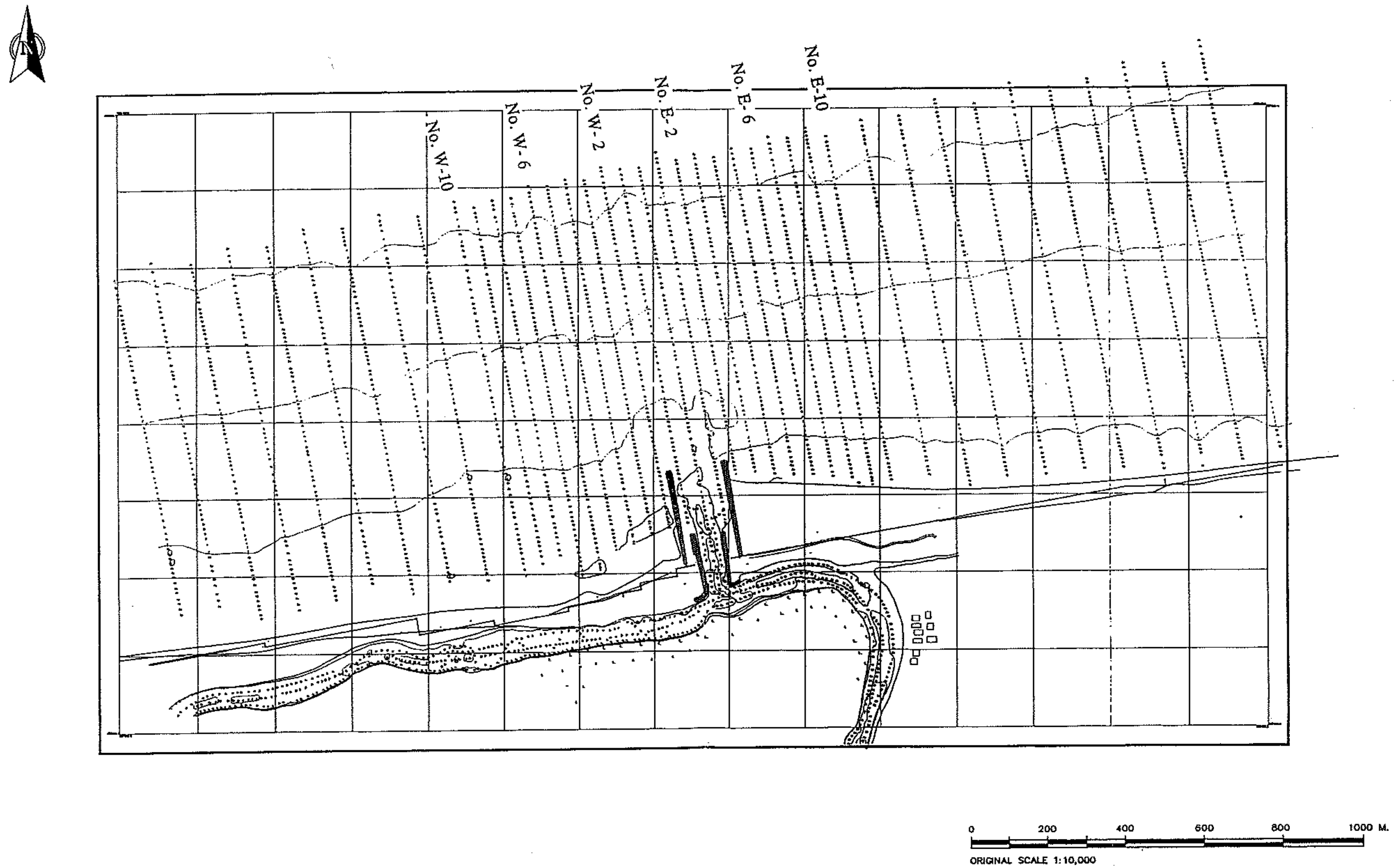

Figure 8.2.1-2 Topographic and Bathymetric Survey Line in Bang Ra Pha Area

On the assumption that the shoreline change was not large before the construction of jetties, the deposition and erosion near the jetties are considered to have occurred during these two years.

The amount of deposition and/or erosion was calculated as 800 m distance on both sides from the jetty because of the limit of survey area of the existing map. Actual areas of deposition and/or erosion are confirmed to be wider than this by site survey.

Assuming the area and volume of deposition and erosion are two times as much as the calculated values, the amount of deposition at east side of jetties becomes about 45,000 m^3/year and the amount of erosion at west side of jetties becomes about 32,000 m^3/year.

Table 8.2.1-1 Amount of Deposition and Erosion in Bang Ra Pha Area

(Year 1996 – 2001)

No. of Survey Line	Cross-Sectional Area (m^2)	Mean Cross-Sectional Area (m^2)	Survey Line Interval (m)	Amount of Deposition/ Erosion (m^3)	Accumulated Amount of Deposition/ Erosion (m^3)
East Side					
No. E-10	– 62.5				
		– 17.5	50.0	– 875.0	– 875.0
No. E- 9	27.5				
		22.5	50.0	1,125.0	250.0
No. E- 8	17.5				
		67.5	50.0	3,375.0	3,625.0
No. E- 7	117.5				
		152.5	50.0	7,625.0	11,250.0
No. E- 6	187.5				
		185.0	50.0	9,250.0	20,500.0
No. E- 5	182.5				
		133.8	50.0	6,687.5	27,187.5
No. E- 4	85.0				
		128.8	50.0	6,437.5	33,625.0
No. E- 3	172.5				
		220.0	50.0	11,000.0	44,625.0
No. E- 2	267.5				
Total	995.0	892.5	400.0	44,625.0	44,625.0
West Side					
No. W- 2	125.0				
		87.5	50.0	4,375.0	4,375.0
No. W- 3	50.0				
		– 8.8	50.0	– 437.5	3,937.5
No. W- 4	– 67.5				
		– 95.0	50.0	– 4,750.0	– 812.5
No. W- 5	– 122.5				
		– 115.0	50.0	– 5,750.0	– 6,562.5
No. W- 6	– 107.5				
		– 106.3	50.0	– 5,312.5	– 11,875.0
No. W- 7	– 105.0				
		– 125.0	50.0	– 6,250.0	– 18,125.0
No. W- 8	– 145.0				
		– 140.0	50.0	– 7,000.0	– 25,125.0
No. W- 9	– 135.0				
		– 125.0	50.0	– 6,250.0	– 31,375.0
No. W-10	– 115.0				
Total	– 622.5	– 627.5	400.0	– 31,375.0	– 31,375.0

Note : Amount of Deposition/ Erosion : + : Deposition
–: Erosion

East Side of Jetties

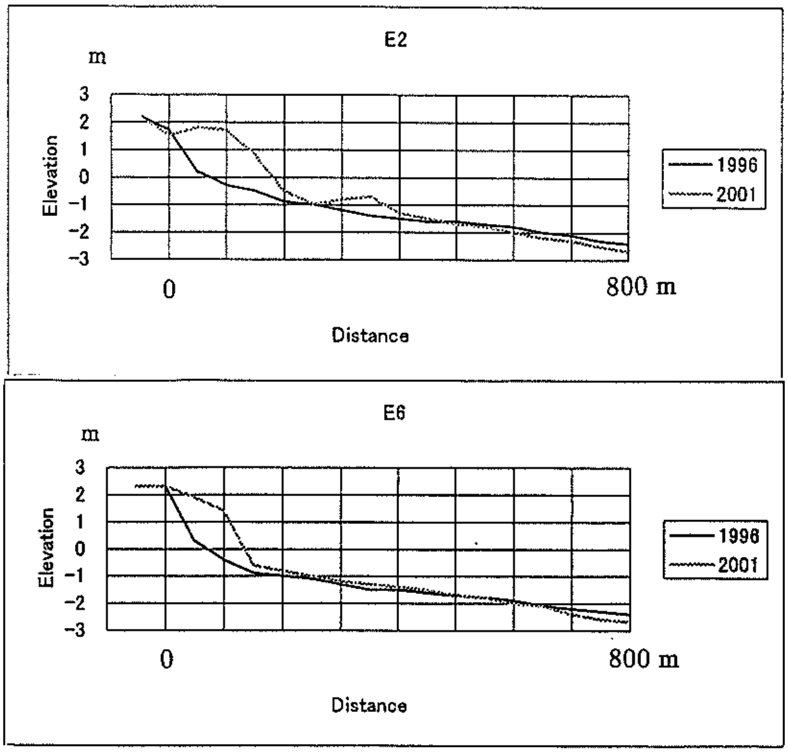

West Side of Jetties

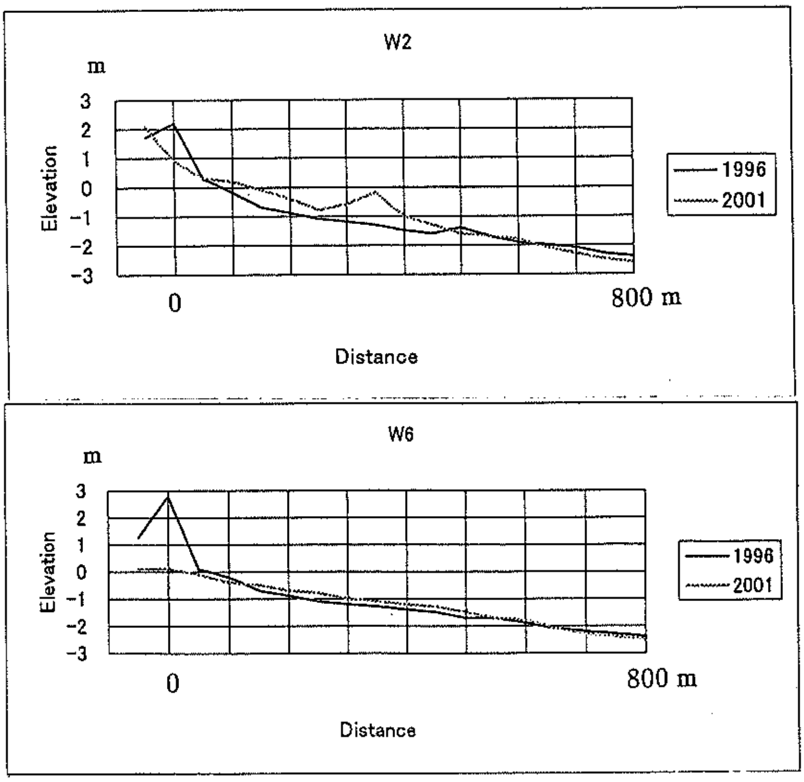

Figure 8.2.1-3 Topographical Cross-Sections in Bang Ra Pha Area

8.2.2 Analysis of Shoreline Changes by Topographic Survey (In Case of Panare and Narathiwat)

For shoreline changes near the attached breakwaters after construction of jetties, the cases in Panare and Narathiwat are shown in Figures 8.2.2-1 and 8.2.2-2 as typical examples.

The details of construction and dimensions of structures in Panare and Narathiwat are shown in Table 8.2.2-1.

Table 8.2.2-1 Construction Year and Dimensions of Structures in Panare and Narathiwat

Item	Panare	Narathiwat
Jetty	Dual Jetties	Dual Jetties
Length of Jetties	250 m and 350 m	350 m and 700 m
Completion Year	July 2001	August 1996
Erosion Control Facility	Detached Breakwaters	Groins (T-type)
Completion Year	November 2000	–
Number of Facilities	Four	Four
Length of Facilities	50 m	50 m
Longshore Spacing	250 m	200 m
Offshore Spacing	25 m – 115m	25 m – 50m
Opening Width	200 m	150 m

In Figures 8.2.2-1 and 8.2.2-2, we can see the predicted shorelines before the construction of detached breakwaters and existing shorelines surveyed in September 2001 during the second phase study.

There is a large difference between the predicted shorelines and the existing shorelines in both areas. And the shoreline shapes in Panare and Narathiwat are almost same except the first detached breakwater area where the dredging sands were dumped. It is said that the existing shoreline looks like a parabolic curve or logarithmic spiral.

Figure 8.2.2-3 shows the details of shoreline shapes of down-coast erosion area in Panare and Narathiwat. The possible extent of erosion in both areas were calculated as follows:

(1) In Case of Panare

Opening Width of Detached Breakwaters (a) : 200 m

Present Maximum Eroded Length (b) : 75 m

Possible Eroded Length (c) : 100 m

Maximum Indentation Factor (c/a) = 0.5

Possible Eroded Length (c) = 0.5 x 200 m

(2) In Case of Narathiwat

Opening Width of T-type Groins (a) : 150 m

Present Maximum Eroded Length (b) : 70 m

Possible Eroded Length (c) : 75 m

Maximum Indentation Factor (c/a) = 0.5

Possible Eroded Length (c) = 0.5 x 150 m

Scale 1 : 5,000

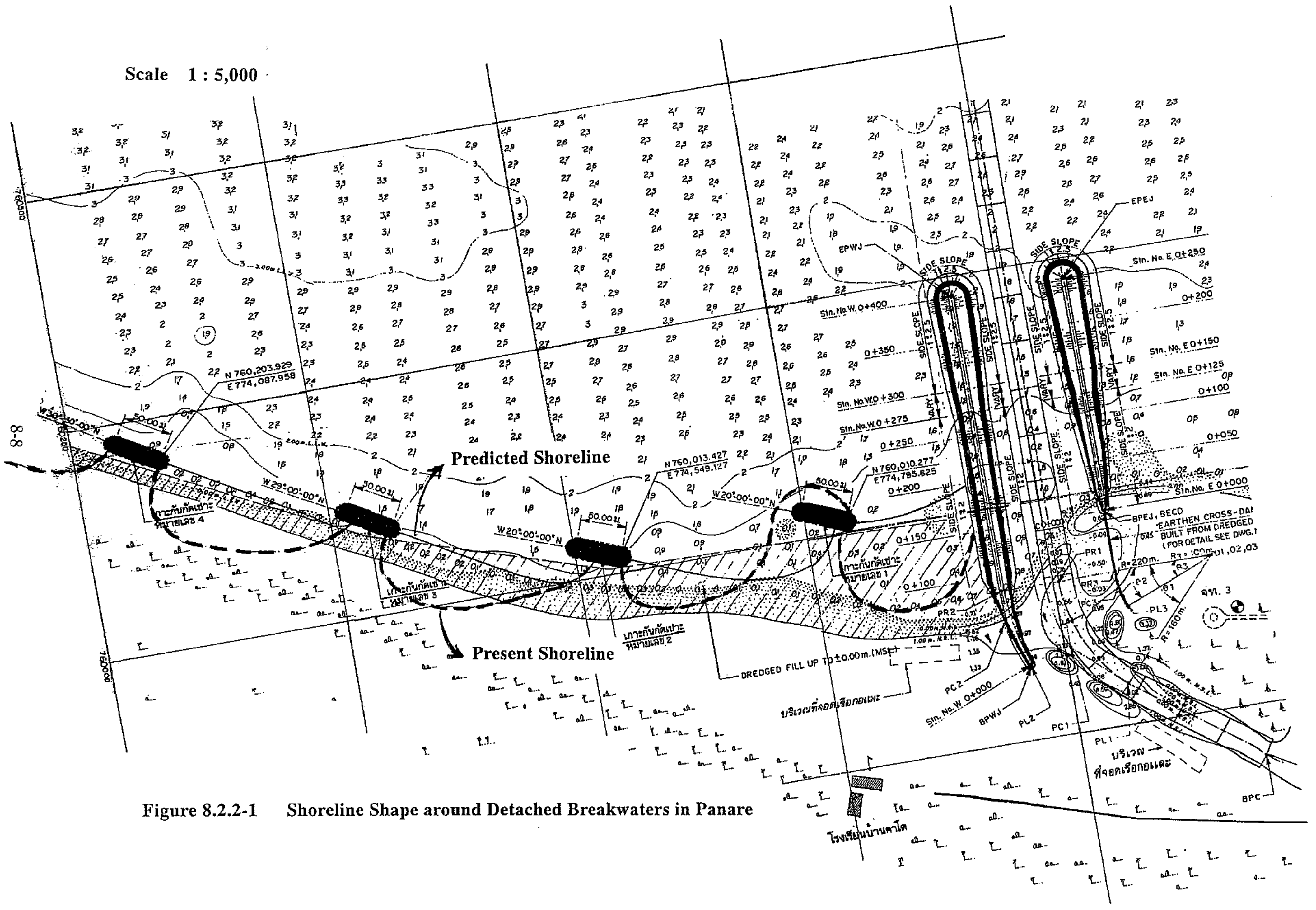

Figure 8.2.2-1 Shoreline Shape around Detached Breakwaters in Panare

Scale 1 : 5,000

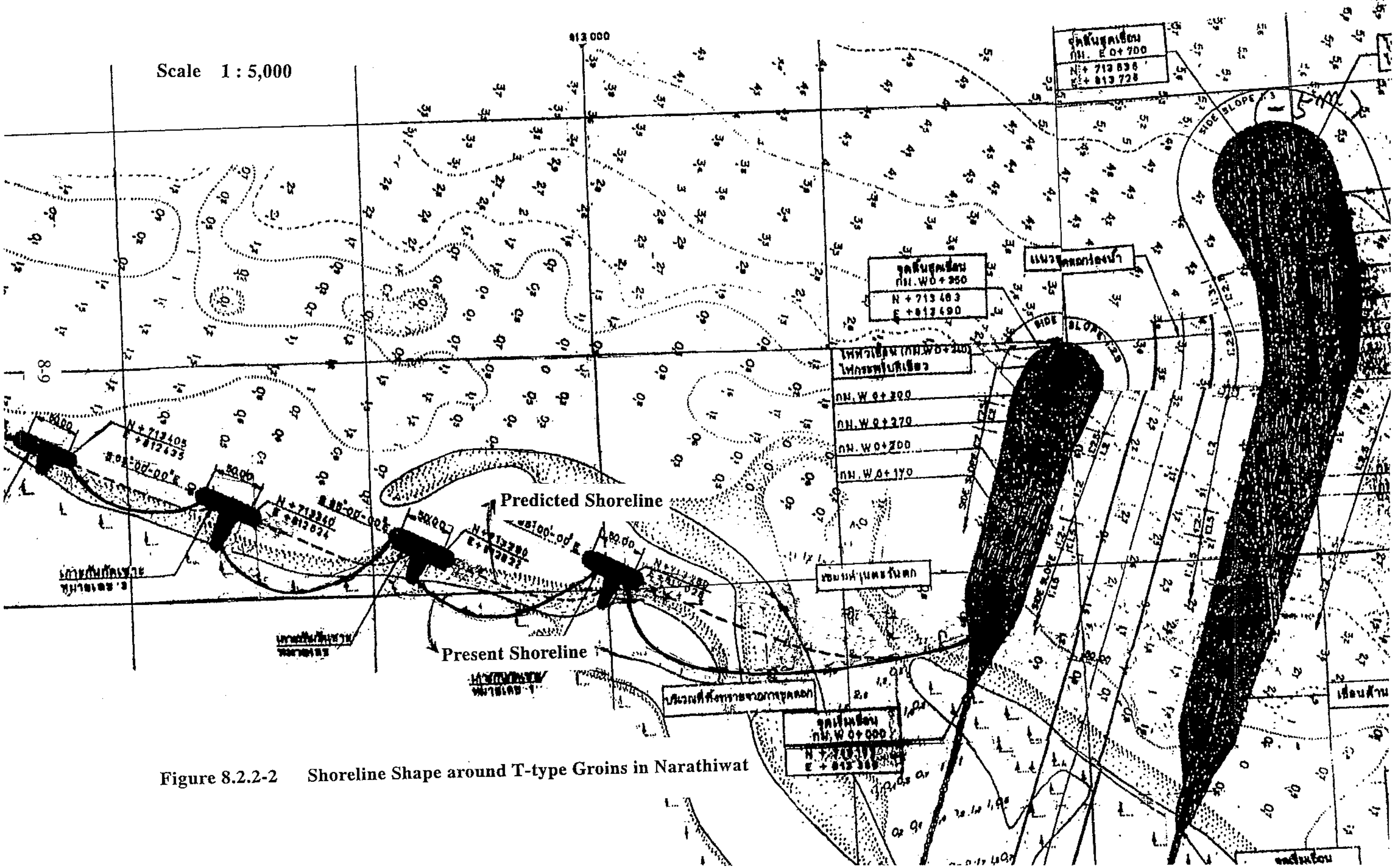

Figure 8.2.2-2 Shoreline Shape around T-type Groins in Narathiwat

(a) Shoreline Shape of Down-coast Erosion Area in Panare

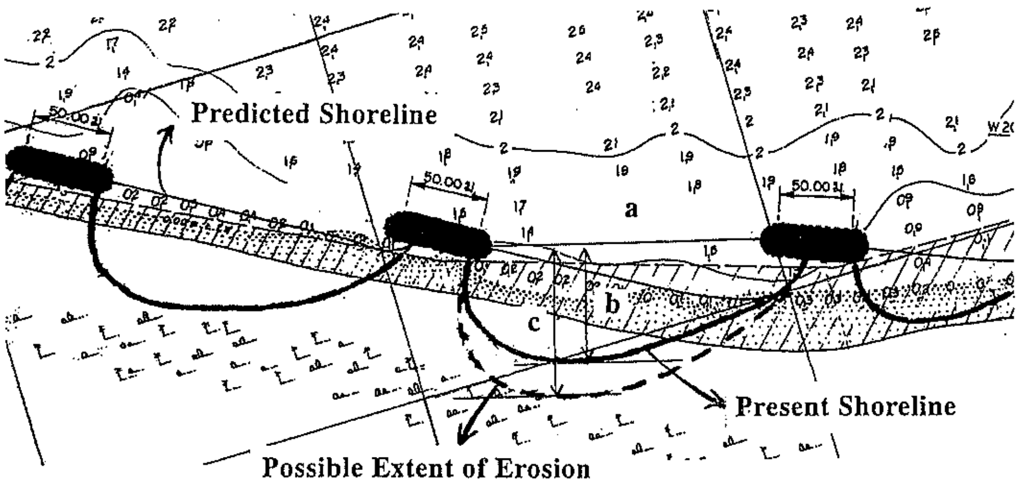

(b) Shoreline Shape of Down-coast Erosion Area in Narathiwat

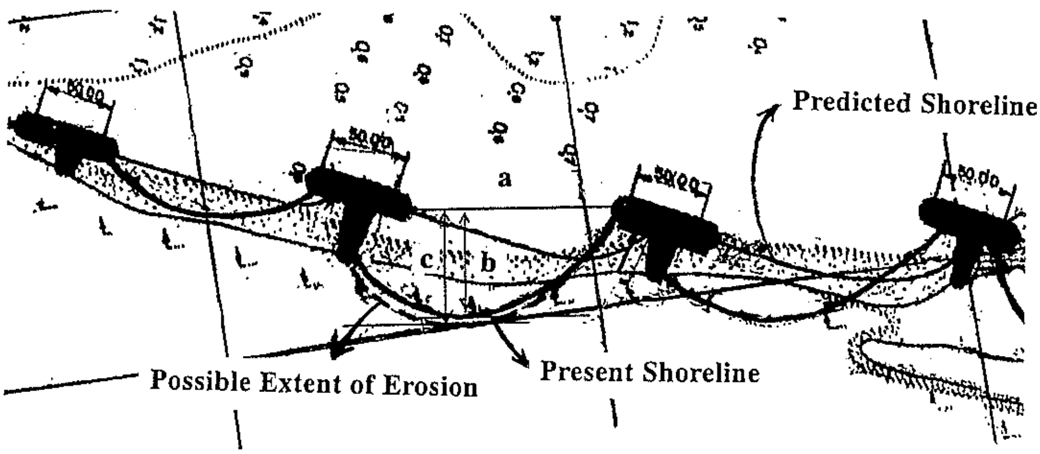

Scale 1 : 5,000

Figure 8.2.2-3 Possible Extent of Erosion in Panare and Naratiwat

8.2.3 Analysis of Topographical Changes by Numerical Simulation

The numerical model for predicting topographical changes in this section consists of three sub-models. At first, the wave field in the objective region is calculated based on a so-called unsteady mild slope equation. Then wave-induced current is calculated together with the mean water level by the shallow water equations. Finally, the change in water depth is estimated numerically through the continuity equation of sediment transport where the local sediment transport rate is evaluated by using calculated wave field and wave-induced current.

(1) Coordinate System and Definitions of Variables

The coordinate system and definitions of the variables used in the numerical model are shown in Figure 8.2.3-1.

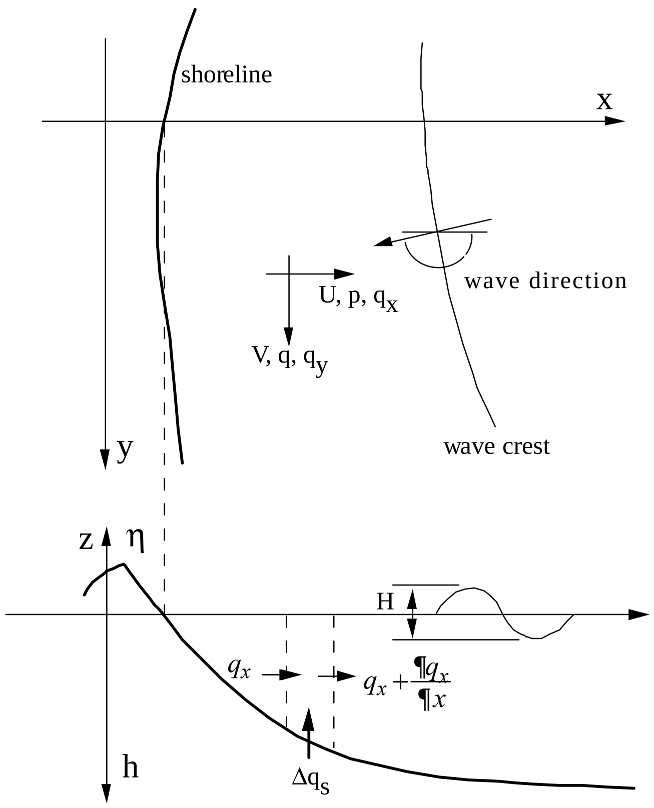

Figure 8.2.3-1 Coordinate System and Definitions of Variables

H,T: wave height and period

è : wave direction

h : surface displacement

U,V : wave-induced depth averaged current velocities in x and y direction

Q=(p,q) : depth integrated mass flux associated with wave motion

(qx,qy) : Local sediment transport rate in x and y directions

Dqs : vertical sediment flux at the bottom (positive in upward direction)

(2) Calculation of Wave Field

a) Fundamental Equations

The equations of motion and continuity are expressed as follows (Nishimura,1983):

$$\frac{¶\boldsymbol{Q}'}{¶t} + \boldsymbol{c}^2\nabla h = 0 \qquad (1)$$

$$\frac{¶h}{¶t} + \frac{1}{n}\nabla\left(n\boldsymbol{Q}'\right) = 0 \qquad (2)$$

$\boldsymbol{Q}'$: vector of depth integrated dischage

h: surface displacement

$\boldsymbol{c}$:wave celelity vector

n= $c_g / |\boldsymbol{c}|$,c_g:group velocity

By using these equations, we can predict wave transformation due to shoaling, diffraction refraction, reflection and breaking in an arbitrary region including structures of arbitrary reflection coefficient.

In the prediction, these equations are transformed into finite differential equations and solved numerically. The so-called Staggard mesh method and Reep-fog method are used to discretize space and time derivatives. The arrangement of variables is shown in Figure 8.2.3-2.

To judge whether waves break or not, the following wave breaking condition is used:

$$|\boldsymbol{Q}'| \geq a\,|\boldsymbol{c}|, a \approx 0.3 \qquad (3)$$

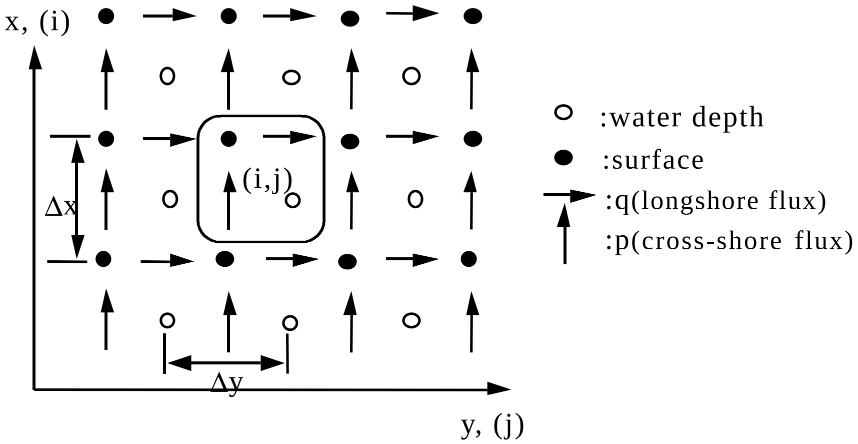

Figure 8.2.3-2 Arrangement of variables in differential scheme

The momentum loss after breaking is assumed to be proportional to the instantaneous momentum at the wave breaking point.

b) Boundary Conditions

Incident waves at offshore boundary (x_o,y_o) is given by the following form:

$$h_i = \frac{H_i}{2}\sin(kx_0\cos q_i + ky_0\sin q_i - wt) \qquad (4)$$

where,

k : the wave number at (x_o,y_o)

s : the angular frequency

H_i and q_i : the incident wave height and angles

Along the side boundary of wave incidence, the surface displacements with phase lag are given. The so-called through boundary condition and arbitrary reflection condition are applied to the another side boundary and around the structures in the calculation region.

The reflection coefficient from jetties and offshore and detached breakwaters are assumed to be 0.4 as the average reflection coefficient from the rubble mound structures.

In this numerical simulation, surface displacement and horizontal mass flux are calculated at grid points of the spacing Dx=Dy=5m and time increment Dt =0.5s.

(3) Calculation of Wave-Induced Current

a) Fundamental Equations

A time and depth averaged N-S equation (the so-called shallow water equation) and equation of mass continuity are used for simulating wave-induced current and mean water level.

Continuity of mass flux:

$$\frac{\partial \bar{h}}{\partial t} + \frac{\partial}{\partial x}\left\{u\left(h+\bar{h}\right)\right\} + \frac{\partial}{\partial y}\left\{v\left(h+\bar{h}\right)\right\} = 0 \qquad (5)$$

Continuity of momentum flux (shallow water equation):

$$\frac{\partial u}{\partial t} + u\frac{\partial u}{\partial x} + v\frac{\partial u}{\partial y} + \frac{1}{r\left(h+\bar{h}\right)}\left(\frac{\partial S_{xx}}{\partial x} + \frac{\partial S_{xy}}{\partial y}\right) = -g\frac{\partial \bar{h}}{\partial x} - \frac{\overline{t_x}}{r\left(h+\bar{h}\right)} + L'\nabla^2 u \qquad (6)$$

$$\frac{\partial v}{\partial t} + u\frac{\partial v}{\partial x} + v\frac{\partial v}{\partial y} + \frac{1}{r\left(h+\bar{h}\right)}\left(\frac{\partial S_{xy}}{\partial x} + \frac{\partial S_{yy}}{\partial y}\right) = -g\frac{\partial \bar{h}}{\partial y} - \frac{\overline{t_{yx}}}{r\left(h+\bar{h}\right)} + L'\nabla^2 v \qquad (7)$$

where,

S_{xx}, S_{xy} and S_{yy} : radiation stress tensors

$\bar{t}_x$ and $\bar{t}_y$: time averaged bottom shear stresses in x and y direction caused by wave and current

L : lateral mixing coefficient

The radiation stress is evaluated from the following expressions using calculated surface displacement:

$$S_{xx} = r\int_{-d}^{0}\overline{u^2}dz + S_0,\ S_{yy} = r\int_{-d}^{0}\overline{v^2}dz + S_0,\ S_{xy} = S_{yx} = r\int_{-d}^{0}\overline{uv}dz \qquad (8)$$

$$S_0 = \frac{1}{2}rg\overline{h^2} - r\int_{-d}^{0}\overline{w^2}dz$$

where,

u, v and w : the water particle velocity in x, y and z direction

These are approximately estimated by the following relations:

$$u = \frac{\partial}{\partial x} f \approx \frac{w}{k} \frac{\cos k(d+z)}{\sinh kd} \frac{\partial h}{\partial x}$$

$$v = \frac{\partial}{\partial y} f \approx \frac{w}{k} \frac{\cos k(d+z)}{\sinh kd} \frac{\partial h}{\partial y}$$

$$w = \frac{\partial}{\partial z} f \approx w \frac{\cos k(d+z)}{\sinh kd} h \qquad (9)$$

For the lateral mixing coefficient and time averaged bottom shear stress, popular expressions by Longet-Higgins are used:

$$L' = \frac{Nh\sqrt{gh}}{\tan b} \qquad (10)$$

$$\bar{\tau}_x = \frac{r}{2} \frac{f_w F_c^2}{(U^2+V^2)^{1/2}} U \,,\; \bar{\tau}_y = \frac{r}{2} \frac{f_w F_c^2}{(U^2+V^2)^{1/2}} V \qquad (11)$$

$$F_c = \frac{U_w^2}{2} + \frac{(U^2+V^2)}{4}$$

where,

N : empirical coefficient (=0.01)

U_w : water particle at the bottom and

f_w : Jonsson's friction factor

To evaluate the value of f_w, approximate expression derived by Swat of the following form is used.

$$f_w = \exp\{-5.977 + 5.113(a_m / k_s)^{-0.194}\} \qquad (12)$$

where,

a_m : excursion of water particle at the bottom

k_s : equivalent roughness height (=2.5*d_{50})

These equations are transformed into differential equations at the same grid points shown in Figure 8.2.3-2 and are solved ADI method (alternating direction implicit method) at time interval Dt=0.5s.

Along offshore and both side boundaries the through boundary condition are applied and the moving boundary condition is used on the shore-ward boundary. In the case where there is river discharge in the calculation region, the river flow is given at the land-ward boundary by surface elevation.

(4) Calculation of Topographic Changes

a) Fundamental Equations

Change in the water depth caused by waves and current is calculated based on the continuity equation of sediment transport in the following form:

$$\frac{\partial h}{\partial t} = \frac{1}{1-l}\left\{-Q_s + \left(\frac{\partial}{\partial x}\left(q_{bx} + e\left|q_{bx}\right|\frac{\partial h}{\partial x}\right) + \frac{\partial}{\partial y}\left(q_{by} + e\left|q_{by}\right|\frac{\partial h}{\partial y}\right)\right)\right\} \qquad (13)$$

where q_{bx}, q_{by} are the local cross-shore and longshore bed load sediment transport rates, e is the empirical coefficient *l* is the void ratio and D Q_s is the spatial gradient of suspended sediment flux that is expressed by using local suspended sediment transport rate q_{sx} and q_{sy}:

b) Local Sediment Transport Rate

$$\Delta Q_s = \frac{\partial q_{sx}}{\partial x} + \frac{\partial q_{sy}}{\partial y} \qquad (14)$$

The bed load transport rate is evaluated by the semi-empirical formula based on power model in the following form:

$$q_{bx} = \frac{e_b}{\tan f(r_s - r)g}\left|\overline{t_{bx}}\right|U$$

$$q_{by} = \frac{e_b}{\tan f(r_s - r)g}\left|\overline{t_{by}}\right|V \qquad (15)$$

where,

e_b : efficiency (=0.12)

r_s : density of bed material and

f : angle of repose of bed material ($\tan f = 0.6$)

The suspended sediment transport rate is estimated by the so-called flux model:

$$q_{sx} = CU, q_{sy} = CV \qquad (16)$$

where *C* is the depth and time averaged suspended sediment concentration that is obtained as the solution to the following advection dispersion equation:

$$\frac{\partial C}{\partial t} + U\frac{\partial C}{\partial x} + V\frac{\partial C}{\partial y} = \frac{\partial}{\partial x}\left(K_x \frac{\partial C}{\partial x}\right) + \frac{\partial}{\partial y}\left(K_y \frac{\partial C}{\partial y}\right) + \frac{1}{h+h} Q_s \qquad (17)$$

where K_x, K_y are the dispersion coefficients in x and y directions, Q_s is the vertical sediment flux from the bottom and is expressed by the following equation using the reference concentration at the bottom C_o, the bottom shear stress u_* and the settling velocity of bed material w_f.

$$Q_s = \left[(1-g)C_o w_f \left(1 - \frac{u_*}{w_f}\right) + C w_f\right] \qquad (18)$$

$$u_* > w_f : \quad g = 0$$

$$u_* < w_f : \quad g = 1$$

For the reference concentration, the expression derived by Deguchi et al. is used.

$$C_o = 0.347 \cdot N_c^{1.77} \qquad (19)$$

$$N_c = \frac{0.688 \hat{u}_w{}^2}{1.33(r_s / r - 1) g w_f T}$$

Equation (17) is transformed into difference scheme at the same grid point shown in Figure 8.2.3-1 and is also solved by ADI method.

(5) Calculation Conditions

The calculation of wave-induced currents and topographic changes was performed for the present condition of structures and future cases in Songkhla, Sichon and Bang Ra Pha areas using the calculation conditions shown in Table 8.2.3-1.

With respect to the future cases of port facilities in Songkhla, Sichon and Bang Ra Pha areas, we assumed the development of port such as expansion of berths, reclamation for container yard and an additional jetty/breakwater in Songkhla, one additional jetty in Sichon and doubling the length of existing jetties in Bang Ra Pha.

Concerning the wave conditions, we assume that the calculation wave was H_0 = 1.0 m, (T_0 = 8.0 sec) and continued for ten hours from the same direction as one storm.

Table 8.2.3-1 Calculation Conditions

Area	Structure	Wave Direction	Remarks
Songkhla	1. Present Case	1. NE + 30° 2. NE – 30°	River Water Level : +1 m (River Flow :50cm/sec)
	2. Future Case Expansion of Berth Additional Jetty	1. NE + 30° 2. NE – 30°	River Water Level : +1 m (River Flow :50cm/sec)
Sichon	1. Present Case	1. ENE + 30° 2. ENE – 30°	
	2. Future Case Additional Jetty	1. ENE + 30° 2. ENE – 30°	700 m
Bang Ra Pha	1. Present Case	1. N + 30° 2. N – 30°	
	2. Future Case Expansion of Jetties	1. N + 30° 2. N – 30°	Double Length (500 m)

(6) Calculation Results

The detailed calculation of topographic changes as well as wave-induced current was carried out for the present case and future case in the feasibility study areas of Songkhla, Sichon and Bang Ra Pha.

a) Songkhla

The current pattern and topographic change in Songkhla area are shown in Figures 8.2.3-3 and 8.2.3-4 for the present case and future case, respectively.

In Songkhla port area, a tranquil sea is made near the jetty area because of offshore islands. However, a wide erosion area is clearly seen in the east side of the existing breakwater.

b) Sichon

The current pattern and topographic change in Sichon area are shown in Figures 8.2.3-5 and 8.2.3-6 for the present case and future case, respectively.

In Sichon area, the deposition volume decreases within the jetties in the future case of constructing an additional jetty comparing with the present case.

c) Bang Ra Pha

The current pattern and topographic change in Bang Ra Pha area are shown in Figures 8.2.3-7 and 8.2.3-8 for the present case and future case, respectively.

In Bang Ra Pha area, the deposition volume decreases within the jetties in the future case of making the length of existing jetties double comparing with the present case as shown in detail in next section (see Table 8.2.3-2).

a) **Wind Direction from NE+ 30°**

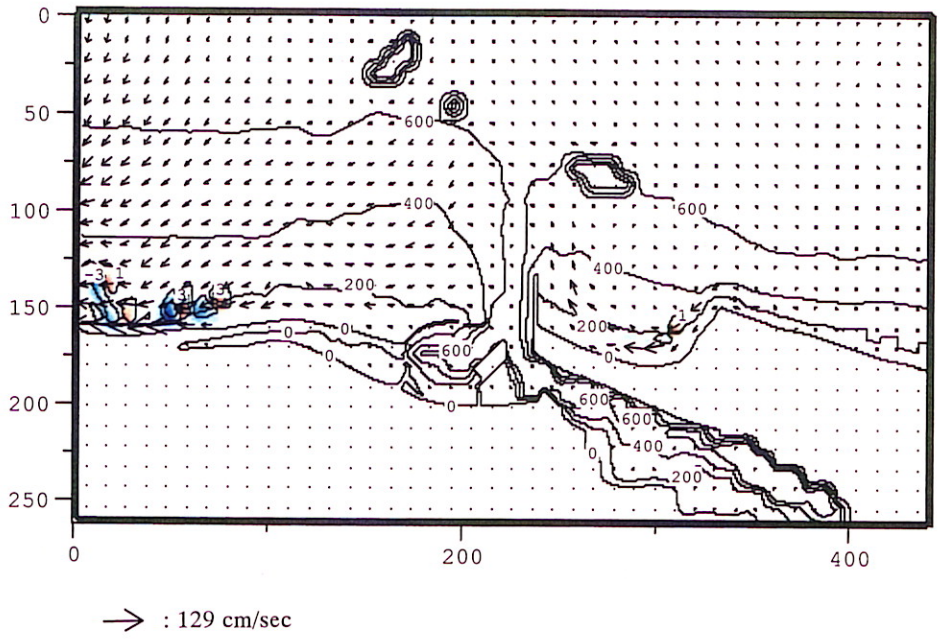

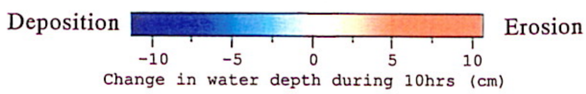

b) **Wind Direction from NE- 30°**

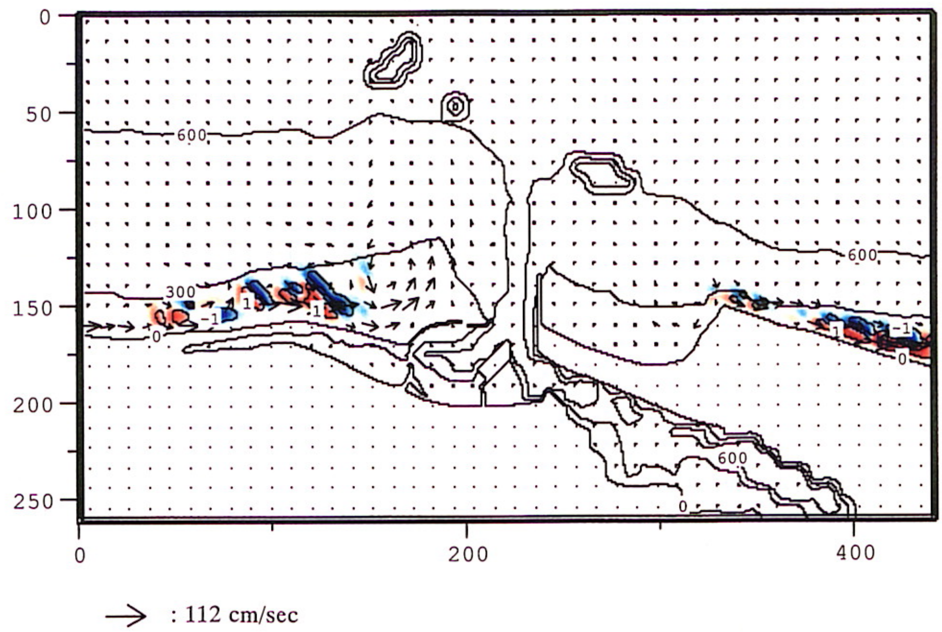

Figure 8.2.3-3 Current Pattern and Topographic Change in Songkhla Area (Present Case)